Cancer Chemother Pharmacol (2012) 70:213–220
DOI 10.1007/s00280-012-1899-6

ORIGINAL ARTICLE

Combination of a MEK inhibitor at sub-MTD with a PI3K/mTOR inhibitor significantly suppresses growth of lung adenocarcinoma tumors in Kras$^{G12D\text{-}LSL}$ mice

Brett H. Simmons · Joseph H. Lee · Kush Lalwani · Anand Giddabasappa · Brittany A. Snider · Anthony Wong · Patrick B. Lappin · Jeetendra Eswaraka · Julie L. Kan · James G. Christensen · Farbod Shojaei

Received: 8 February 2012 / Accepted: 20 May 2012 / Published online: 9 June 2012

Abstract The role of PI3K and MAPK pathways in tumor initiation and progression is well established; hence, several inhibitors of these pathways are currently in different stages of clinical trials. Recent studies identified a PI3K/mTOR (PF-04691502) and a MEK inhibitor (PD-0325901) with strong potency and efficacy in different cell lines and tumor models. PD-0325901, however, showed adverse effects when administered at or above MTD (maximum tolerated dose) in the clinic. Here, we show in preclinical models that PD-0325901 at doses well below MTD (sub-MTD 1.5 mg/kg SID) is still a potent compound as single agent or in combination with PF-04691502. We first observed that PD-0325901 at 1.5 mg/kg SID and in combination with PF-04691502 (7.5 mg/kg; SID) significantly inhibited growth of H460 (carry Kras and PIK3CA mutations) orthotopic lung tumors. Additionally, we tested efficacy of PD-0325901 in Kras$^{G12D\text{-}LSL}$ conditional GEMMs (genetically engineered mouse models) which are a valuable tool in translational research to study tumor progression. Intranasal delivery of adenoviruses expressing Cre recombinase (Adeno-Cre) resulted in expression of mutant Kras leading to development of tumor lesions in lungs including adenomatous hyperplasia, large adenoma, and adenocarcinoma. Similar to H460 tumors, PD-0325901 as single agent or in combination with PF-04691502 significantly inhibited growth of tumor lesions in lungs in Kras$^{G12D\text{-}LSL}$ mice when treatment started at adenocarcinoma stage (at 14 weeks post-Adeno-Cre inhalation). In addition, immunohistochemistry showed inhibition of pS6 (phosphorylated ribosomal S6) in the treated animals particularly in the combination group providing a proof of mechanism for tumor growth inhibition. Finally, m-CT imaging in live Kras$^{G12D\text{-}LSL}$ mice showed reduction of tumor burdens in PD-0325901-treated animals at sub-MTD dose. In conclusion, our data suggest that PD-0325901 at doses below MTD is still a potent compound capable of tumor growth inhibition where Kras and/or PI3K are drivers of tumor growth and progression.

Keywords PI3K pathway · MAPK pathway · Lung tumor · Combination therapy

Brett H. Simmons and Joseph H. Lee equally contributed to this work.

B. H. Simmons · J. H. Lee · J. L. Kan · J. G. Christensen · F. Shojaei (✉)
Oncology Research Unit, Pfizer Global R&D,
10724 Science Center Dr., La Jolla, San Diego, CA 92121, USA
e-mail: Farbodshojaei@hotmail.com

K. Lalwani · A. Giddabasappa · J. Eswaraka
Department of Comparative Medicine, Pfizer Global R&D,
10724 Science Center Dr., La Jolla, San Diego, CA 92121, USA

B. A. Snider · A. Wong · P. B. Lappin
Department of Drug Safety Research & Development,
Pfizer Global R&D, 10724 Science Center Dr.,
La Jolla, San Diego, CA 92121, USA

Introduction

The superfamily of PI3K (phosphoinositide 3-kinase) plays a fundamental role in homeostasis by regulating several key cellular activities such as proliferation, metabolism, and survival [1, 2]. To the same extent, deregulation of PI3K pathway due to genetic abnormalities such as mutation or amplification of components of the pathway (particularly PIK3IA) is frequently observed in several human cancers. Among four classes of PI3K family, class IA consists of a regulatory subunit (members of p85) and a catalytic subunit (p110α) known to be more frequently involved in cancer occurrence and progression [3, 4].

Kras mutation is one of the major drivers of tumor progression in several cancer types including NSCLC (non-small cell lung cancer) [5], pancreatic carcinomas [6], and CRCs (colorectal carcinoma) [7]. Therefore, $Kras^{G12D\text{-}LSL}$ genetically engineered mouse model (GEMM) may be one of the most relevant models to study tumor growth and progression in NSCLC and testing the efficacy of anti-cancer compounds [8]. Recent investigations suggest that $Kras^{G12D\text{-}LSL}$ GEMM may closely mimic the clinical trial outcome in cancer patients [9].

Activated Kras also has the ability to bind to p110α resulting in the activation of PI3K pathway. mTORC1 & 2 (mammalian target of rapamycin containing protein complex) are also involved in the activation of PI3K-AKT that in turn results in the activation of downstream cellular functions [10, 11]. Although Ras has the ability to activate PI3K pathway, inhibition of PI3K pathway in established tumors in Kras-mutated lung model does not completely inhibit tumor growth indicating role of other signaling pathways such as MAPK in the growth of NSCLCs [12]. Inhibition of PI3K/mTOR pathway may result in the activation of MAP kinase pathways through compensatory mechanisms. Similarly, treatment of Kras-mutant cancer cell lines with MEK inhibitor may activate the PI3K pathway leading to lack of response to the treatment [13]. Given the role of MAPK and PI3K in the progression of a variety of tumor types including NSCLC, pancreatic ductal carcinoma, and CRC, several inhibitors of the above pathways are in different stages of clinical trials [1, 14, 15], particularly dual inhibitors of PI3K and mTOR pathways as they appear to be more effective than selective inhibitors to block mTOR pathway when it is activated independent of PI3K [14, 16]. Recent investigations identified PF-04691502 (hereafter PF-502) as a potent dual inhibitor of PI3K/mTOR [17] and PD-0325901 (hereafter PD-901) as an inhibitor of MEK pathway [18]. A recent report showed anti-tumor activity of PF-502 in several preclinical models [19], while PD-901 has shown potent tumor growth inhibition in papillary thyroid carcinoma cells [20]. Very recent report in a GEMM of ovarian cancer ($Kras^{G12D\text{-}LSL}Pten^{-/-}$) showed that combination of PD-502 and PD-901 significantly inhibited tumor growth and increased survival compared with either monotherapy [21].

Despite potent anti-tumor activity, PD-901 administration in patients at 15 mg or higher has been associated with several adverse effects including visual disturbances secondary to retinal vein occlusion (RVO) [22–24]. In an effort to alleviate potential toxicity without compromising anti-tumor efficacy, we tested efficacy of combination therapy using PD-901 at sub-MTD dose (1.5 mg/kg) in a human xenograft cell line (NCI-H460) and also in $Kras^{G12D\text{-}LSL}$ mice. Our investigations indicate that PD-901 is still a potent inhibitor of MAPK pathway even at doses below MTD as single agent and particularly in combination with PF-502.

Materials and methods

Tumor implantation

All animal experimentation was approved by the Pfizer La Jolla Institutional Animal Care and Use Committee (IACUC). Human H460-Luc (luciferase) expressing cells were grown in RPMI1640 supplemented with 10 % FCS. Cells were injected iv (intravenous via tail vein) in Scid/beige mice (1×10^6 in 200 µl PBS). Mice were randomized at 7 days after implantation when tumors were established in the lungs and were treated with Vehicle, PF-502 (7.5 mg/kg; SID, MTD: 10 mg/kg [19]), PD-901 (1.5 mg/kg; SID, MTD: 25 mg/kg [24]) and combination of both compounds. For Luc imaging, mice were injected intraperitoneally with luciferin (at randomization stage 15 mg/ml and for other time points 3 mg/ml, Promega, WI) and were anesthetized with isoflurane. Anesthetized animals were imaged in a Xenogen IVIS-100 instrument (Caliper Biosciences, MA, USA). Luc signals were normalized to 1,000–30,000 counts/s, analyzed and quantified using Living Image 4.0 Software (Caliper, MA).

Tumor development in $Kras^{G12D\text{-}LSL}$ GEMMs

$Kras^{G12D\text{-}LSL}$ heterozygous mice were obtained from Jackson Laboratories (Jax West, CA) at approximately 3–4 weeks of age. Lung tumors were generated in $Kras^{G12D\text{-}LSL}$ mice, using a previously published protocol developed by DuPage et al. [25]. Adenovirus expressing Cre recombinase (Adeno-Cre) was purchased from the University of Iowa Gene Transfer Vector Core. Viral titration was determined by Adenoviral Titration Kits (Clontech, CA) using the manufacturer's protocol. Mice were administered with 2.5×10^7 infectious units (IU) of the adenovirus by inhalation. Prior to inhalation, Adeno-Cre (2.5×10^7 IU) was prepared in 50 µl media (MEM, Gibco BRL; Life Sciences, CA) containing 10 mM CaCl2 followed by incubation at room temperature (RT) for 20 min. $Kras^{G12D\text{-}LSL}$ mice were anesthetized using Ketamine and Xylazine and the Adeno-Cre preparation was administered intranasally. Using the above procedure, we were able to consistently and reproducibly generate tumors in $Kras^{G12D\text{-}LSL}$ mice. To ensure tumor formation and progression, $Kras^{G12D\text{-}LSL}$ mice ($n = 1$–3) were euthanized at several time points (4, 8, 12 and 16 weeks post-inhalation) and lung tissues were fixed in formalin. Sections of lungs were stained with H&E (Hematoxylin and Eosin) using standard protocols provided by Department of Drug Safety Research

and Development (DSRD). In a series of studies, we observed that using our optimized method, tumors were approximately distributed evenly in the lung. In addition, using serial sectioning, it was evident that the distribution of tumors was consistent between the surface and the parenchyma of the lung tissue, providing us with the confidence to analyze a single lobe of lung possibly as a representative of the entire organ.

To score lesions (hyperplastic, benign adenoma, and adenocarcinoma) in each lung, all the H&E slides were analyzed by a certified pathologist who was provided detail of the study design and the treatments. Hyperplastic lesions were defined by increased density in alveolar epithelial cells with uniform size and shape and no evident mitotic activity. Adenoma lesions were clusters of alveolar epithelial cells that were monomorphic, hypertrophic and were arranged in multiple layers with papillary extensions. Adenocarcinoma lesions were defined by tumor epithelial cells (generally larger than hyperplastic/adenoma cells) in different size and shape that were clustered in papillary forms or dense sheets.

Therapeutic compounds

At 8 weeks post-inhalation, lung tissues were isolated from the $Kras^{G12D\text{-}LSL}$ recipient mice to ensure tumor formation. Treatment with anti-cancer agents was initiated at 14 weeks after inhalation with Adeno-Cre when lung lesions are at advanced stage (adenocarcinoma) of tumorigenesis in $Kras^{G12D\text{-}LSL}$ mice (3, 5). Tumor-bearing mice were treated with anti-cancer compounds including Pfizer selective mTOR inhibitor hereafter PSMI; 80 mg/kg; SID); PF-502 (7.5 mg/kg; SID); PD-901 (1.5 mg/kg; SID); combination of PF-502 and PD-901 at the respected dose; two standard of care regimens including CarbPac (combination of Carboplatin, 75 mg/kg; Strem Chemicals, MA, and Paclitaxel, 15 mg/kg; Teva, CA); and GemCis (combination of Gemcitabine, 112 mg/kg; Eli Lilly, IN and Cisplatin, 4 mg/kg; Sigma, CA). Treatments were terminated after 8 weeks and lung lesions were analyzed.

m-CT (micro-computed tomography)

$Kras^{G12D\text{-}LSL}$ mice were administered with Adeno-Cre by inhalation as described. Mice received treatments including vehicle, PF-502, PD-901, and combination at 19.5 weeks post-inhalation and at doses described above. For m-CT imaging and at 4 weeks after treatment initiation, mice were anesthetized using isoflurane inhalation and were imaged at 15 min post-administration of ExiTron nano 12,000 (Miltenyi Biotech, CA). All images were acquired in standard resolution using respiratory gating (70 kVP, 114 μA, 300 ms integration time, 41 μm voxel size). Images were saved as 2D binary digital imaging communication (DICOM) files and later were analyzed using third-party DICOM image processing applications 64-bit OsiriX v.3.9.2 (Pixmeo; Switzerland) and/or Analyze v.10.0 (AnalyzeDirect; Overland Park, KS, USA).

Results

Combination of PF-502 and PD-901 inhibits tumor growth in H460 lung colonization model

The H460 cell line that carries mutations in Kras and PIK3CA has been widely used in a variety of in vitro and in vivo studies [26]. To test the efficacy of PF-502 and PD-901 in a NSCLC model and in order to monitor tumor progression and response to therapy, mice were iv injected with H460-Luc line. At day-7 post-injection, mice were randomized to treatment groups once Luc signal was detected and was quantified to select a cohort of mice for efficacy study (Fig. 1a). In addition to PF-502, PD-901, and combination of both agents, we also included two SOC (standard of care) regimens including CarbPac and GemCis in the treatment groups. Quantification of Luc signals in H460 tumors at three different time points post-treatment suggested that combination of PF-502 and PD-901 has greater tumor growth inhibition compared with either monotherapy (Fig. 1b). Our data also indicate that daily administration of PD-901 in the combination regimen at 1.5 mg/kg was not associated with any significant adverse effects or deaths during the course of treatment. Additionally, between the two SOC regimens, GemCis showed superior efficacy compared with CarbPac and the corresponding control (Fig. 1c). However, both SOC regimens were associated with some adverse effects in the recipients. In conclusion, our data in H460-Luc tumors are the first study to show that PD-901 is potent at sub-MTD dose to inhibit tumor growth and invasiveness when used in combination with an inhibitor of PI3K/mTOR.

Combination of PF-502 and PD-901 at sub-MTD dosing significantly inhibited growth of adenocarcinoma lung tumors in $Kras^{G12D\text{-}LSL}$ mice

To further validate H460-Luc tumor data, we tested efficacy of combination regimen in $Kras^{G12D\text{-}LSL}$ mice using the same therapeutic regimens described for the H460-Luc tumor models. $Kras^{G12D\text{-}LSL}$ mice have been widely used for variety of tumor biology studies [8]. The conditional nature of $Kras^{G12D}$ activation allows tumor initiation in any tissue where Kras is a driver of tumor progression. Generation of lung tumors was one of the original studies in $Kras^{G12D\text{-}LSL}$ mice where intranasal inhalation of adenoviral expressing Cre recombinase (Adeno-Cre) resulted in the

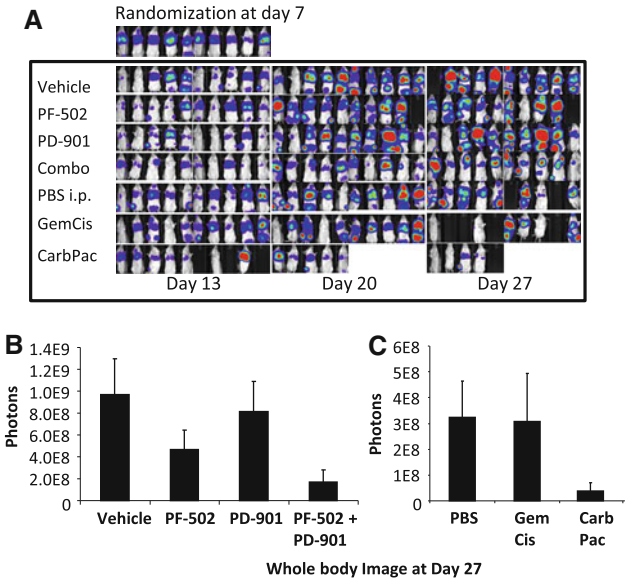

Fig. 1 **a** Scid/beige mice were iv implanted with human H460-Luc + cells (1×10^6 per mouse). Mice were imaged at day-7 post-implantation and were randomized to 7 groups ($n = 10$) receiving vehicle, PF-04691502, PD-0325901, combination of PF-04691502 and PD-0325901, injectable PBS, two standard of care regimens including CarbPac and GemCise. Treated animals were imaged in IVIS-100 system weekly for 3 consecutive weeks. **b**, **c** Quantification of photons of lungs in tumor bearing mice at last time point (day 27) treated with small molecule inhibitors (**b**) or standard of care (**c**)

expression of $Kras^{G12D}$ in the lung and formation of adenomatous hyperplasia, papillary adenoma, large adenoma, and adenocarcinoma at different time points post-inhalation [8, 25]. Following the same methodology, we provided a strategy to develop tumors in $Kras^{G12D}$ mice and to treat them with our compounds. As depicted in Fig. 2a, $Kras^{G12D}$ mice were administered with Adeno-Cre (2.5×10^7) and lung lesions were analyzed in few mice at 8 weeks post-inhalation to ensure tumor initiation and progression. At 14 weeks post-inhalation when most of recipients have developed adenocarcinoma lesions [8, 25], mice were assigned to therapeutic regimens and the study was terminated at 22 weeks post-inhalation. Following the above strategy, and at 14 weeks post-inhalation, $Kras^{G12D}$ mice received the same treatments as H460-Luc study. To differentiate role of PI3K versus mTOR pathway, a selective mTOR inhibitor was also included in the regimens. Analysis of lung tissues showed that while PF-502 or PD-901 alone had the ability to inhibit growth of majority of adenocarcinoma lesions, combination therapy significantly suppressed adenocarcinoma lesions further suggesting that PD-901 at sub-MTD dose might have therapeutic benefit in NSCLC tumors (Fig. 2b). Similar to the results with the H460-Luc model, SOC regimens inhibited tumor growth in $Kras^{G12D}$ mice. Analysis of body weight in the treated animals did not reveal any significant difference between PD-901 (as single agent or in combination)- and vehicle-treated mice further suggesting lack of adverse effect when administering the compound at sub-MTD.

Combination of PF-502 and PD-901 significantly inhibits growth of all lung lesions

To further investigate detail of efficacy of combination regimen, lung lesions were classified as hyperplastic, benign adenoma, or adenocarcinoma and were quantified in each mouse and in each treatment in histopathology analyses (Fig. 3a). Interestingly, PSMI (selective mTOR inhibitor)-treated lungs had very few benign adenoma like lesions but there was no significant change in the total percentage of all lesions These data suggest that tumor initiation and progression in $Kras^{G12D}$ mice is independent of mTOR pathway. PF-502 as a single agent significantly inhibited the percentage of all three lesions in the lung compared with vehicle-treated animals. Strikingly, PD-901 as a single agent and at sub-MTD dose also significantly inhibited all three lesions in the lung further suggesting a strong potency for the compound even at levels significantly below MTD (Fig. 3b). Combination of PF-502 and PD-901 suppressed the percentage of all three lesions in the lung further validating human H460 tumor data. Lesion classification also allowed us to investigate frequency of each lesion in the recipients (Fig. 3c). Irrespective of type of treatment, all animals carried hyperplastic lesions indicating that none of the therapies can fully eradicate tumor initiation and progression in the recipients. Interestingly and despite efficacy as single agent in inhibiting percentage of adenoma lesions, PF-502 or PD-901 monotherapies did not completely inhibit the adenoma lesions. However, PSMI, combination regimen and SOCs reduced the percentage of mice carrying adenoma lesions. PD-901 as single agent or in combination with PF-502 showed superior efficacy in reducing frequency of mice carrying adenoma lesions. Finally, with the exception of vehicle and PSMI, all other treatments reduced percentage of mice carrying adenocarcinoma lesions. PD-901 as single agent or in combination with PF-502 showed superior efficacy in reducing frequency of mice with adenocarcinoma lesions (Fig. 3c). In conclusion, quantification of lesions further suggested a great potency for PD-901 at sub-MTD dose as single agent or in combination with PF-502.

Combination of PF-502 and PD-901 significantly inhibits phosphorylation of ribosomal S6 (pS6) protein in $Kras^{G12D\text{-}LSL}$ mice

To investigate whether superior efficacy of PD-901 correlates with inhibition of downstream signaling pathway,

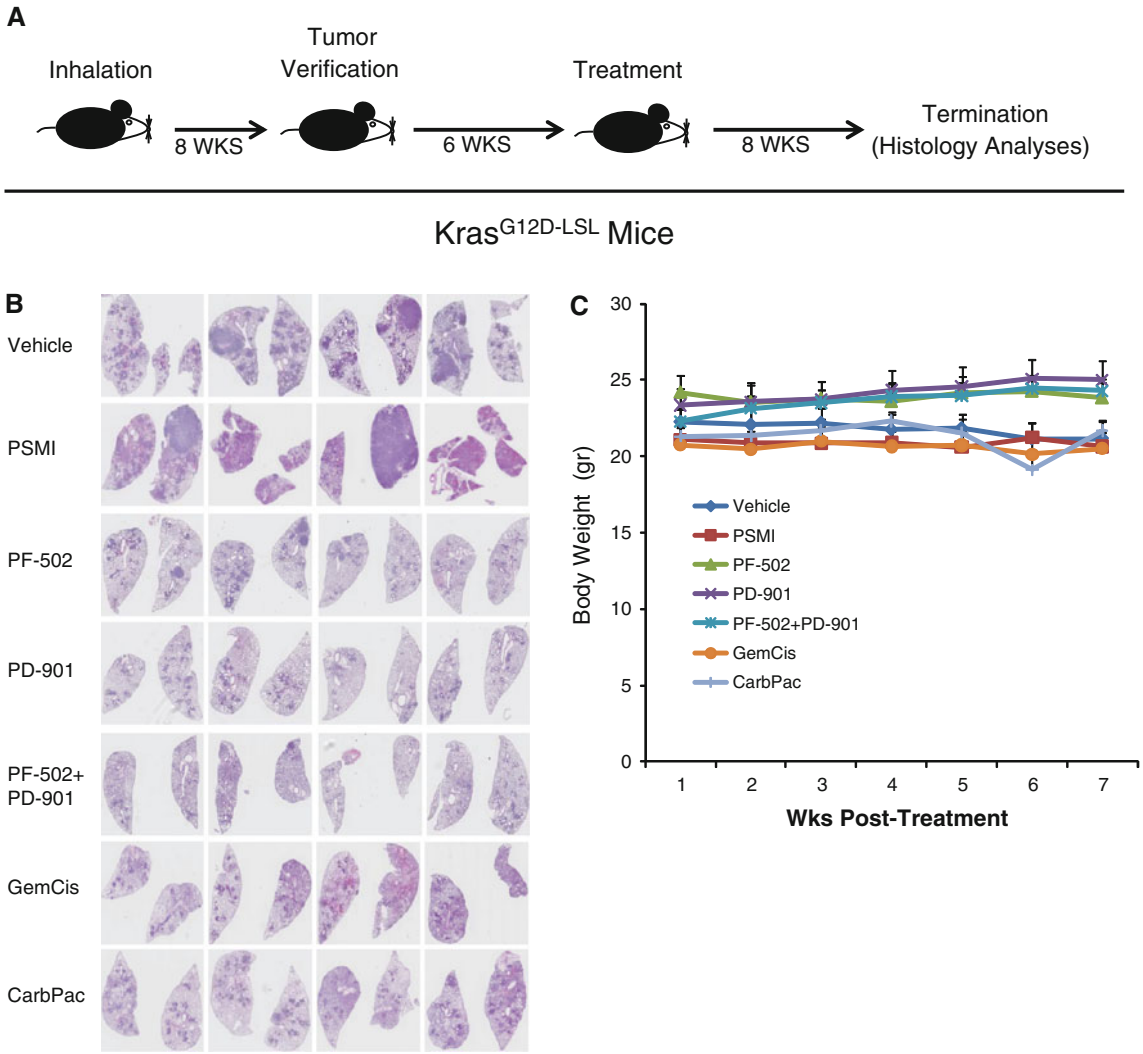

Fig. 2 **a** A Strategy to investigate tumor progression and response to therapy in $Kras^{G12D\text{-}LSL}$ GEMMs. Mice would be administered (inhalation) with Adeno-Cre virus (2.5×10^7) as described and few mice would be analyzed at 8 weeks post-adeno-inhalation to ensure tumor progression in the lung. At 14 weeks post-inhalation, mice would be assigned to treatment with the compounds as described in the Methods. All the treated mice would be killed after 8 weeks (i.e. 22 weeks after Adeno-cre inhalation) and one lobe of lung tissue would be analyzed in histology using H&E staining. **b** Using our strategy, $Kras^{G12D\text{-}LSL}$ mice were administered with Adeno-Cre and received therapeutic compounds at 14 weeks post-inhalation followed by study termination and tissue analysis. Each image is representative of lung from one mouse, i.e., images of lung from 4 mice from each treatment are shown. Combination of PI3K/mTOR and MEK inhibitors has the most potent effect on tumor growth inhibition (reduced sub-gross lung tumor burden; manifested as dense, dark blue regions in the lung tissue) compared with all other treatments. **c** Body weights were measured in all the recipients once/week. Administration of PD-901 did not significantly change body weight versus all other treatments

phosphorylation status in ribosomal S6 protein was investigated in lung sections [19]. As illustrated in Fig. 4, pS6 signal was observed in majority of lesions in vehicle-treated tumors, indicative of pathway activation. PF-502 or PD-901 as single agent partially inhibited the signal in tumor cells; however, combination regimen fully inhibited pS6 in tumors further providing a correlation between tumor growth and pathway activation. These studies suggest that PD-901 potency and efficacy at sub-MTD dose is selectively associated with inhibition of the downstream signaling pathway.

m-CT technology further verifies efficacy of combination of PF-502 and PD-901 therapy in live mice

One of the major caveats of adenovirus delivery of Cre recombinase is the lack of a reporter in the vector in order to horizontally monitor tumor progression in the mice. Additionally, given the transient nature of gene expression in any adenoviral expressing system, inclusion of any reporter in the adenoviral expressing Cre would not provide a permanent expression to monitor tumor growth at advance stages of tumorigenesis. For these reasons,

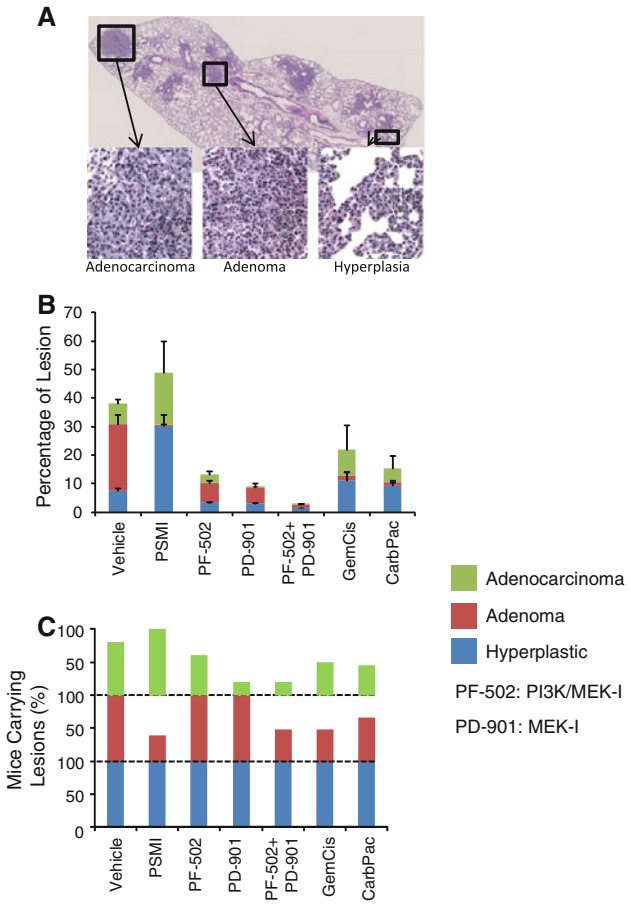

Fig. 3 Lesion classification to quantify percentage of lesions in lung in each mouse. $Kras^{G12D\text{-}LSL}$ mice were administered and treated as described in Fig. 2a. **a** Representative lesions (hyperplastic, benign adenoma, and adenocarcinoma) are shown in a lung tissue. **b** Percentage of lung occupied by each lesion type was quantified in each mouse and averaged for each treatment group. **c** Percentage of mice exhibiting each lesion in each treatment to investigate whether therapeutic compounds have the ability to fully inhibit tumor growth in the recipients. *Bars* represent percentage of mice bearing each lesion in the lung. While all the treated mice exhibit hyperplastic lesions, only 20 % of animals treated with combination of PI3K/mTOR and MEK inhibitors display adenocarcinoma lesions in the lung

development of other imaging modalities would provide a great approach in monitoring tumor progression and response to the therapies. Among several imaging techniques, m-CT has proven to be a reliable method to image lung tumors at different stages of tumorigenesis [27]. To further confirm efficacy of PD-901 at sub-MTD dose as single agent or in combination regimen and to further gain confidence in efficacy study, we treated mice at ~19.5 weeks after inhalation where majority of lung is covered by tumor lesions. Image analysis of whole lungs at 4 weeks after the treatment clearly shows tumor regions in the vehicle-treated mice compared with non-inhaled animals (Fig. 5a). Consistent with histology data, PF-502 partially inhibited tumor growth, whereas PD-901 showed a better efficacy as monotherapy (Fig. 5b). Combination regimen provided a superior efficacy compared with monotherapies and further confirmed histology and lesion classification data (Fig. 5b, c).

Discussion

Here, we examined the efficacy of PD-901 at a sub-MTD dose in two different lung tumor models where conditional/spontaneous activation of mutated Kras (in both $Kras^{G12D\text{-}LSL}$ mice and H460 tumor cells) and PIK3CA (in H460 tumor cells) are major drivers of tumorigenesis. In order to mimic clinical status where most patients are diagnosed and receive therapies at advance stage of tumorigenesis, treatments started when tumors were established in H460 model or at advanced stage (adenocarcinoma) in $Kras^{G12D\text{-}LSL}$ GEM. Efficacy data as well as animals overall health (as measured by body weight) suggested an excellent potency for PD-901 as a single agent or in combination with PF-502 that was well-tolerated by the recipients. Combination therapy significantly suppressed tumor growth in both H460-Luc and $Kras^{G12D\text{-}LSL}$ tumors; however, PD-901, as a single agent, had superior efficacy in the latter suggesting that PIK3CA is a major driver of tumorigenesis in the former. Comparison of two SOCs also showed that the overall efficacy of CarbPac was greater in both models compared with GemCis further raising a question about the mechanism of action in lung tumors between the two regimens. Detailed analysis of lesions in the $Kras^{G12D\text{-}LSL}$ tumors showed that inhibition of mTOR alone may not provide a benefit, while the dual inhibitor (PF-502) significantly inhibited growth of all 3 lesions in the lung. Future studies using a selective PI3K inhibitor will determine whether, compared with dual inhibitors, suppression of PI3K is sufficient to inhibit tumor growth in $Kras^{G12D\text{-}LSL}$ mice. Interestingly, PD-901 as a single agent was very efficacious in inhibiting tumor progression in $Kras^{G12D\text{-}LSL}$ mice further emphasizing the significance of targeting the driver of tumorigenesis (i.e., MEK pathway) in this model. Analysis of lung lesions in individual mice showed that none of the therapies eliminated the development of hyperplastic lesions further confirming that tumors may not be fully prevented or reversed by any treatment. Adenoma and adenocarcinoma lesions were most affected by combination regimen indicating an active cross-talk between MEK and PI3K at this stage of tumorigenesis. To investigate whether downstream signaling pathway is also targeted by the therapies, IHC data showed that pS6 is almost fully inhibited only in the combination group correlating efficacy data and activity of signaling pathways in $Kras^{G12D\text{-}LSL}$ tumors. Finally, m-CT imaging of live mice treated with PD-901

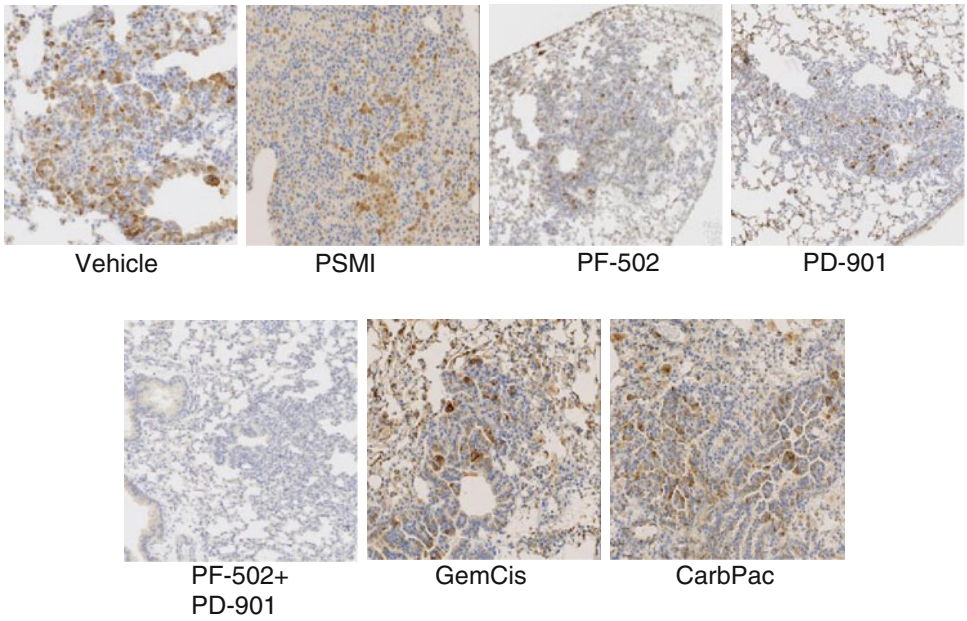

Fig. 4 $Kras^{G12D\text{-}LSL}$ mice were administered with Adeno-Cre and were treated as described above. Sections of lungs were stained with pS6 antibody using optimized protocol provided in the laboratory. Among all the treatments, combination of PF-502 and PD-901 has significantly inhibited S6 phosphorylation

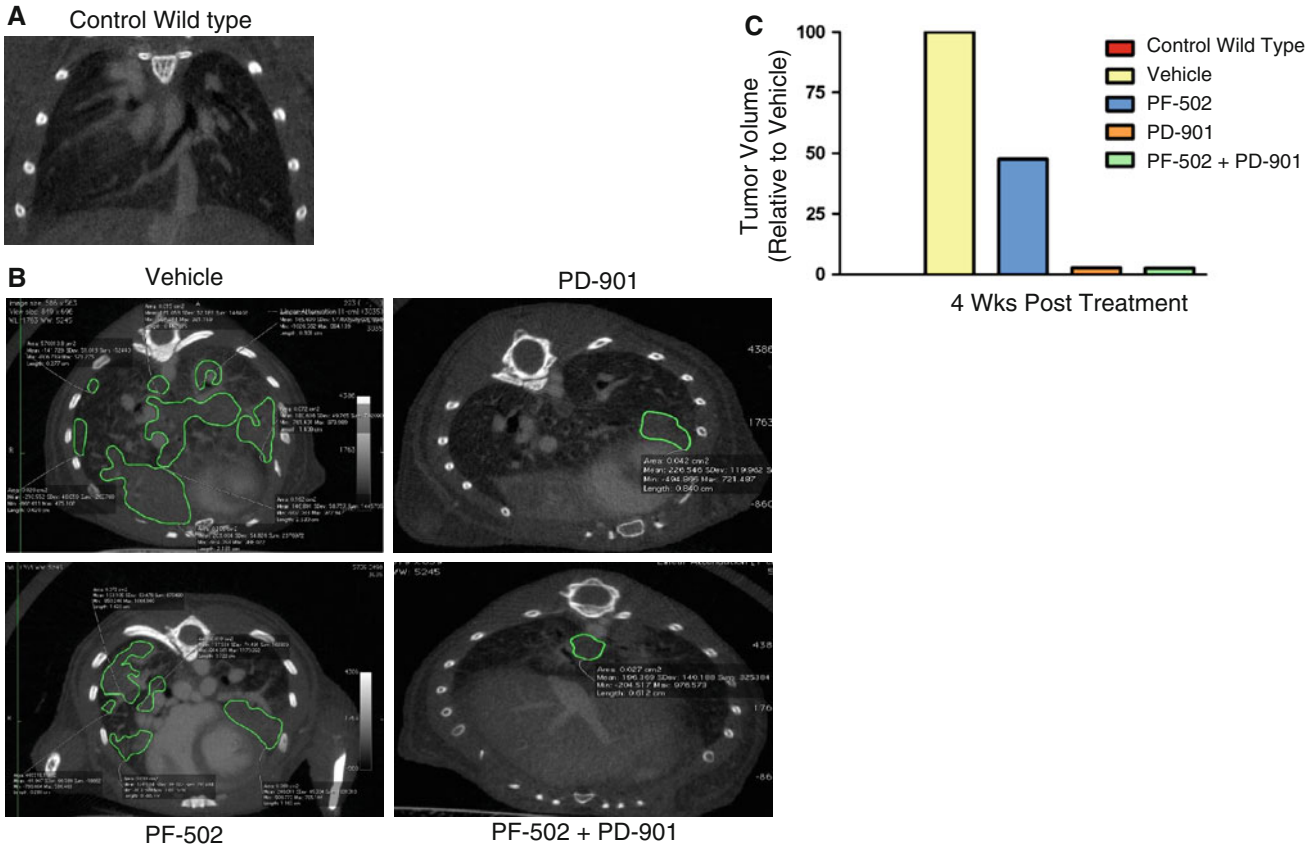

Fig. 5 m-CT images further support efficacy of PD-901 as single agent or in combination regimen in treated animals. $Kras^{G12D\text{-}LSL}$ mice were administered with Adeno-Cre as described and received treatments (vehicle, PF-502, PD-901 and PF-502 + PD901) at ~ 19.5 weeks post-inhalation. M-CT images were taken from control wild type (**a**) and $Kras^{G12D\text{-}LSL}$ mice (**b**) at 4 weeks after the treatment. **c** Quantification of tumor volume (relative to vehicle) in control wild type and treated mice is included

and PF-502 at an advance stage of tumor progression (~19.5 weeks post-inhalation) exhibited reduced lesion size, further supporting IHC data. Overall, our investigations indicate that PD-901 is a potent compound at doses significantly below the established MTD but without previously reported major adverse effects in the recipients and suggest

that therapeutic compounds might be very efficacious at lower dose if they are administered in cancers with targeted mutations/pathway activation. Future studies will determine clinical benefit of combination of PF-502 and PD-901 in cancer patients.

References

1. Engelman JA, Luo J, Cantley LC (2006) The evolution of phosphatidylinositol 3-kinases as regulators of growth and metabolism. Nat Rev Genet 7:606–619
2. Kuruvilla FG, Schreiber SL (1999) The PIK-related kinases intercept conventional signaling pathways. Chem Biol 6:R129–R136
3. Miled N, Yan Y, Hon WC, Perisic O, Zvelebil M, Inbar Y, Schneidman-Duhovny D, Wolfson HJ, Backer JM, Williams RL (2007) Mechanism of two classes of cancer mutations in the phosphoinositide 3-kinase catalytic subunit. Science 317:239–242
4. Huang CH, Mandelker D, Schmidt-Kittler O, Samuels Y, Velculescu VE, Kinzler KW, Vogelstein B, Gabelli SB, Amzel LM (2007) The structure of a human p110alpha/p85alpha complex elucidates the effects of oncogenic PI3K alpha mutations. Science 318:1744–1748
5. Forbes SA, Bhamra G, Bamford S, Dawson E, Kok C, Clements J, Menzies A, Teague JW, Futreal PA, Stratton MR (2008) The catalogue of somatic mutations in cancer (COSMIC). Curr Protoc Hum Genet. Chapter 10, Unit 10.11
6. Kullmann F, Hartmann A, Stohr R, Messmann H, Dollinger MM, Trojan J, Fuchs M, Hollerbach S, Harder J, Troppmann M, Kutscheidt A, Endlicher E (2011) KRAS mutation in metastatic pancreatic ductal adenocarcinoma: results of a multicenter phase II study evaluating efficacy of cetuximab plus gemcitabine/oxaliplatin (GEMOXCET) in first-line therapy. Oncology 81:3–8
7. Liu X, Jakubowski M, Hunt JL (2011) KRAS gene mutation in colorectal cancer is correlated with increased proliferation and spontaneous apoptosis. Am J Clin Pathol 135:245–252
8. Jackson EL, Willis N, Mercer K, Bronson RT, Crowley D, Montoya R, Jacks T, Tuveson DA (2001) Analysis of lung tumor initiation and progression using conditional expression of oncogenic K-ras. Genes Dev 15:3243–3248
9. Singh M, Lima A, Molina R, Hamilton P, Clermont AC, Devasthali V, Thompson JD, Cheng JH, Bou Reslan H, Ho CC, Cao TC, Lee CV, Nannini MA, Fuh G, Carano RA, Koeppen H, Yu RX, Forrest WF, Plowman GD, Johnson L (2010) Assessing therapeutic responses in Kras mutant cancers using genetically engineered mouse models. Nat Biotechnol 28:585–593
10. Castellano E, Downward J (2011) RAS Interaction with PI3K: more than just another effector pathway. Genes Cancer 2:261–274
11. Shaw RJ, Cantley LC (2006) Ras, PI(3)K and mTOR signalling controls tumour cell growth. Nature 441:424–430
12. Engelman JA, Chen L, Tan X, Crosby K, Guimaraes AR, Upadhyay R, Maira M, McNamara K, Perera SA, Song Y, Chirieac LR, Kaur R, Lightbown A, Simendinger J, Li T, Padera RF, Garcia-Echeverria C, Weissleder R, Mahmood U, Cantley LC, Wong KK (2008) Effective use of PI3K and MEK inhibitors to treat mutant Kras G12D and PIK3CA H1047R murine lung cancers. Nat Med 14:1351–1356
13. Wee S, Jagani Z, Xiang KX, Loo A, Dorsch M, Yao YM, Sellers WR, Lengauer C, Stegmeier F (2009) PI3K pathway activation mediates resistance to MEK inhibitors in KRAS mutant cancers. Cancer Res 69:4286–4293
14. Courtney KD, Corcoran RB, Engelman JA (2010) The PI3K pathway as drug target in human cancer. J Clin Oncol 28:1075–1083
15. Shuttleworth SJ, Silva FA, Cecil AR, Tomassi CD, Hill TJ, Raynaud FI, Clarke PA, Workman P (2011) Progress in the preclinical discovery and clinical development of class I and dual class I/IV phosphoinositide 3-kinase (PI3K) inhibitors. Curr Med Chem 18:2686–2714
16. Yap TA, Garrett MD, Walton MI, Raynaud F, de Bono JS, Workman P (2008) Targeting the PI3K-AKT-mTOR pathway: progress, pitfalls, and promises. Curr Opin Pharmacol 8:393–412
17. Cheng HSB, Bailey S, Edwards M, Hoffman J, Hu Q, Kania R, Knighton DR, Marx MA, Ninkovic S, Sun S, Zhang E (2010) Discovery of the highly potent PI3K/mTOR dual inhibitor PF-04691502 through structure based drug design. MedChemComm 1:139–144
18. Barrett SD, Bridges AJ, Dudley DT, Saltiel AR, Fergus JH, Flamme CM, Delaney AM, Kaufman M, LePage S, Leopold WR, Przybranowski SA, Sebolt-Leopold J, Van Becelaere K, Doherty AM, Kennedy RM, Marston D, Howard WA Jr, Smith Y, Warmus JS, Tecle H (2008) The discovery of the benzhydroxamate MEK inhibitors CI-1040 and PD 0325901. Bioorg Med Chem Lett 18:6501–6504
19. Yuan J, Mehta PP, Yin MJ, Sun S, Zou A, Chen J, Rafidi K, Feng Z, Nickel J, Engebretsen J, Hallin J, Blasina A, Zhang E, Nguyen L, Sun M, Vogt PK, McHarg A, Cheng H, Christensen JG, Kan JL, Bagrodia S (2011) PF-04691502, a potent and selective oral inhibitor of PI3K and mTOR kinases with antitumor activity. Mol Cancer Ther 10:2189–2199
20. Henderson YC, Chen Y, Frederick MJ, Lai SY, Clayman GL (2010) MEK inhibitor PD0325901 significantly reduces the growth of papillary thyroid carcinoma cells in vitro and in vivo. Mol Cancer Ther 9:1968–1976
21. Kinross KM, Brown DV, Kleinschmidt M, Jackson S, Christensen J, Cullinane C, Hicks RJ, Johnstone RW, McArthur GA (2011) In vivo activity of combined PI3K/mTOR and MEK inhibition in a Kras(G12D);Pten deletion mouse model of ovarian cancer. Mol Cancer Ther 10:1440–1449
22. Boasberg PD, Redfern CH, Daniels GA, Bodkin D, Garrett CR, Ricart AD (2011) Pilot study of PD-0325901 in previously treated patients with advanced melanoma, breast cancer, and colon cancer. Cancer Chemother Pharmacol 68:547–552
23. Haura EB, Ricart AD, Larson TG, Stella PJ, Bazhenova L, Miller VA, Cohen RB, Eisenberg PD, Selaru P, Wilner KD, Gadgeel SM (2010) A phase II study of PD-0325901, an oral MEK inhibitor, in previously treated patients with advanced non-small cell lung cancer. Clin Cancer Res 16:2450–2457
24. LoRusso PM, Krishnamurthi SS, Rinehart JJ, Nabell LM, Malburg L, Chapman PB, DePrimo SE, Bentivegna S, Wilner KD, Tan W, Ricart AD (2010) Phase I pharmacokinetic and pharmacodynamic study of the oral MAPK/ERK kinase inhibitor PD-0325901 in patients with advanced cancers. Clin Cancer Res 16:1924–1937
25. DuPage M, Dooley AL, Jacks T (2009) Conditional mouse lung cancer models using adenoviral or lentiviral delivery of Cre recombinase. Nat Protoc 4:1064–1072
26. SangerInstitute, http://www.sanger.ac.uk/
27. Ritman EL (2011) Current status of developments and applications of micro-CT. Annu Rev Biomed Eng 13:531–552